Structural estimation robust to events of extreme sample variation

Alan Ledesma

This version: Jun 2024

Abstract

This paper develops a structural estimation technique within a state-space model framework that is robust to persistent tail events, such as the Covid-19 pandemic. The proposed approach is sufficiently general to handle any event causing significant sample variation, making it valuable in an changing environment characterized by notable uncertainty. The approach is validated through the estimation of a simple semi-structural model of a closed economy using data from the United States, Canada, and the Euro Area. Our findings indicate that the proposed treatment enhances model fit and stabilizes coefficients. It is also found that during the Covid-19 pandemic, significant shock adjustments were observed up to 2020Q4. Finally, omitting the suggested correction leads to underestimated uncertainty, excessive output gap responses, inadequate output trend responses, and biased estimates of unobservable variables.

1 Introduction

The year 2020 has been challenging for the world due to the Covid-19 pandemic. From a macroeconomic perspective, the pandemic triggered unprecedented sample variability in many key macroeconomic variables. These effects, however, varied heterogeneously across sectors and macroeconomic variables. For instance, most countries experienced sharp contractions in economic activity (to varying degrees across sectors), while other variables such as inflation or interest rates appeared unaffected. The notable complexity of this event has diminished the ability to analyze the economy using traditional models.

Moreover, even if we assume the Covid-19 did not induce a regime switch, the substantial sample variability generated significantly complicates estimation, filtering, and forecasting exercises in time series models, especially structural models. Currently, there is no clear consensus on how to appropriately handle macroeconomic data during the pandemic. It remains uncertain whether including pandemic data in inference without any adjustment is reasonable or if it may lead to serious distortions. Specifically, regarding structural models, will the 2020 data introduce bias in coefficient estimation, latent variable filtering or forecasting? And if so, for how long?

This paper aims to extend the Kalman filter to implement estimation robust to the large sample variability observed during the Covid-19 pandemic. This exercise is relevant as it may improve our understanding of the pandemic's economic impacts and also because similar events may occure again in a changing enviroment.[1] Currently, accurately estimating structural models and their corresponding latent variables is challenging, and this document seeks to address this issue.

Specifically, the aim is to develop a technique for structural estimation algorithm within a state-space model framework that can withstand persistent tail events. Several studies have already pursued this goal, primarily concentrating on time series models. Notably, Lenza and Primiceri (2022) (referred to as LP2022 henceforth) and Carriero, Clark, Marcellino, and Mertens (2022) stand out. In these studies, the emphasis lies in improving the estimation of Bayesian Autoregressive models to effectively manage considerable sample variability. Both papers tackle the Covid-19 impact by accommodating surges in state shocks volatility during affected periods, thereby facilitating adaptive adjustments of the algorithm to fit the data.

On the structural estimations side, Morley, Rodríguez-Palenzuela, Sun, and Wong (2023) (based on Kamber, Morley, and Wong (2018)) have leveraged long-term relationship structures in time series models to estimating unobservable variables through and adapted Beveridge-Nelson filter.[2] In their application, the authors implement a variation of LP2022 in the estimation stage of the approach. Another noteworthy effort is by Holston, Laubach, and Williams (2020), HLW2020 from now on.[3] In this paper the Oxford COVID-19 government strigency index is used as a measurable variable to gauge pandemic severity.[4] They also allow for increased measurement error volatility to mitigate pandemic effects on measurement variables. This approach effectively reduces the weight of measurable variables in the estimation, offering a middle ground between excluding pandemic data and fully incorporating it into estimation.

An alternative simple solution could be to discard potential outliers observed in 2020. However, as discussed by LP2022, while this strategy may produce reasonable coefficient estimates, it could introduce biases in forecasting exercises or latent variable filtering, and also lead to an underestimation of uncertainty.

The methodology to elaborate in this paper incorporates elements from LP2022's approach by allowing sudden variance increases during the pandemic, aligning with significant sample variability. However, the focus here is

[1] Such as another pandemic, a major economic crisis (akin to a sunspot for small open economies), or extreme climatological phenomena.
[2] The filter is desscribed in Beveridge and Nelson (1981)
[3] This paper is an extensión of Holston, Laubach, and Williams (2017) and Laubach and Williams (2003).
[4] See Hale, Webster, Petherick, Phillips, and Kira (2020).

on a structural or state-space model. Adapting LP2022's methods to these applications requires careful selection of shocks affected by tail events.

To validate the algorithm, we construct a simple semi-structural model of a closed economy based on HLW2020. This model is sufficiently simple to quickly grasp various transmission mechanisms yet flexible enough to replicate macroeconomic data. We use the same data as HLW2020, specifically from the United States (US), Canada (CA), and the Euro Area (ES). It is important to note that HLW2020 and this paper adopt different approaches regarding pandemic data treatment. Here, we closely follow LP2022's approach, aiming to replicate pandemic-executed data with increased variance in state variables. Conversely, HLW2020 increases measurement error variance, which significantly alters interpretation compared to the discussion above. Additionally, our developed algorithm does not include additional information sources to signal the pandemic, unlike HLW2022.

In the application, it has been observed that the Covid-19 treatment proposed here enhances the model's fit to the data and promotes coefficients stability. The adjustments to the shocks are significant between 2020q1 and 2020q3 but not in 2020q4; therefore, this correction is not applied from 2020Q1 onwards. It is also noteworthy that the Covid-19 treatment eliminates the large variation of state shocks within the system. Regarding the estimation of latent variables, it can be noticed that omitting the Covid-19 correction leads to underestimated uncertainty, excessive response of the output gap, inadequate response of the output trend, resulting in biased estimates of non-observable variables.

This paper is structured as follows: Section 2 presents the extension to the Kalman Filter incorporating the Covid-19 correction in volatility. Section 3 describes the application used in this paper and displays the results. Finally, Section 4 provides the conclusions.

2 An extended Kalman Filter

Following LP2022, it is plausible to associate the data observed during the pandemic with a sudden surge in volatility. Essentially, this assumes that the dynamic interrelations among various macroeconomic variables remain unaltered by the pandemic, thereby suggesting the absence of a regime shift. Given this premise, it becomes feasible to extend the Kalman filter in a straightforward manner to accommodate extreme volatility spikes over brief periods, thereby yielding an estimate that is robust to the sample variability induced by the pandemic. The refined Kalman filter not only computes the state variables but also the likelihood, thereby facilitating the application of conventional estimation techniques either Bayesian or frequentist.

The solution to any linear stochastic dynamic model can be expressed as a state-space representation (Gaussian) with the following features:

$$\begin{aligned} &\text{Space equation} \quad : \quad \mathbf{y}_t = \mathbf{Z}\boldsymbol{\alpha}_t + \mathbf{B}\mathbf{x}_t + \boldsymbol{\varepsilon}_t \qquad \text{with } \boldsymbol{\varepsilon}_t \overset{iid}{\sim} \mathcal{N}(\mathbf{0}, \mathbf{H}) \\ &\text{State equation} \quad : \quad \boldsymbol{\alpha}_t = \mathbf{c} + \mathbf{T}\boldsymbol{\alpha}_{t-1} + \mathbf{R}\boldsymbol{\eta}_t \qquad \text{with } \boldsymbol{\eta}_t \overset{iid}{\sim} \mathcal{N}(\mathbf{0}, \mathbf{Q}_t) \end{aligned} \tag{2.1}$$

where the measurement variables, $\mathbf{y}_t$, and measurement errors, $\boldsymbol{\varepsilon}_t$, are of dimensions $p \times 1$. The vector of exogenous variables, $\mathbf{x}_t$, is of dimension $k \times 1$, the vector of state variables, $\boldsymbol{\alpha}_t$, is $s \times 1$, while the vector of state errors, $\boldsymbol{\eta}_t$, is $r \times 1$. Similarly, the loading matrix, $\mathbf{Z}$, the intercept of states, $\mathbf{c}$, the transition matrix, $\mathbf{T}$, the shock loading matrix, $\mathbf{R}$, the variance of measurement errors, $\mathbf{H}$, and the variance of state shocks, $\mathbf{Q}_t$, are comfortable matrices.

Some measurement variables in 2020 exhibited extraordinary sample variability (e.g., GDP). The proposal made in this paper implies that certain state variables experience a surge in sample variation through a variance increase of their corresponding shocks. In this context, let us assume that the state shocks $\eta_{i,t}$ (for $i \in I$) increase their volatility due to the pandemic, while others do not (i.e., $\eta_{j,t}$ for $j \notin I$). In the state-space system,

$var(\eta_{i,t}) = [Q_t]_{i,i}$, let's further assume $[Q_t]_{i,i} = \kappa_{i,t} q_{i,i}$ where

$$\kappa_{i,t} = \begin{cases} 1, & \text{if } t < t^* \text{ or } t > t^* + \tau^* \\ \bar{\kappa}_{i,\tau}, & \text{if } t = t^* + \tau \text{ for } \tau \in \{0, ..., \tau^*\} \end{cases} \tag{2.2}$$

where t_* is the period in which the pandemic started while τ^* (to be estimated) corresponds to the duration of the event.

Define $\mathbf{s} = \{\bar{s}_{i,\tau}\}_{\tau \leq \tau^*, i \in I}$ as the vector that collects all the parameters necessary to specify $\kappa_{i,t}$. Additionally, define $\boldsymbol{\theta}$ as the coefficients within the matrices $\mathbf{Z}(\boldsymbol{\theta})$, $\mathbf{B}(\boldsymbol{\theta})$, $\mathbf{H}(\boldsymbol{\theta})$, $\mathbf{c}(\boldsymbol{\theta})$, $\mathbf{T}(\boldsymbol{\theta})$, $\mathbf{R}(\boldsymbol{\theta})$ and $\mathbf{Q}_t = \mathbf{Q}(\boldsymbol{\theta}, \mathbf{s}, t)$. With this arrangement, a Bayesian recursion can be implemented.

Conditional to $\mathbf{s}$, the likelihood can be computed with the standard Kalman filter over (2.1). Thus, the posterior density function is

$$p\left(\boldsymbol{\theta}, \mathbf{s} | \mathbf{y}^T\right) \propto p\left(\mathbf{y}^T | \boldsymbol{\theta}, \mathbf{s}\right) p\left(\boldsymbol{\theta}\right) p\left(\mathbf{s}\right) \tag{2.3}$$

The prior distribution for $\boldsymbol{\theta}$ (i.e., $p(\boldsymbol{\theta})$) should keep its standard formulation, that is, with no pandemic considerations. Conversely, the prior distribution for $\mathbf{s}$ (i.e., $p(\mathbf{s})$) can be kept diffuse.[5]

As a result, the Bayesian recursion is the following:

1. **Initialization**: Maximize the posterior distribution function $p\left(\boldsymbol{\theta}, \mathbf{s} | \mathbf{y}^T\right)$ in (2.3) and set $\boldsymbol{\theta}^{(0)} = \hat{\boldsymbol{\theta}}$, $\mathbf{s}^{(0)} = \hat{\mathbf{s}}$, and $\mathbf{L} = \text{chol}(\mathcal{H})$, where $\mathcal{H}$ is the inverse Hessian at the maximum.

2. Set $r = r + 1$ and draw a candidate vector $[\boldsymbol{\theta}^{*\prime}\ \mathbf{s}^{*\prime}]^\prime$ from the following Gaussian random walk proposal function:

$$\begin{bmatrix} \boldsymbol{\theta}^* \\ \mathbf{s}^* \end{bmatrix} = \begin{bmatrix} \boldsymbol{\theta}^{(r-1)} \\ \mathbf{s}^{(r-1)} \end{bmatrix} + c\mathbf{L}\boldsymbol{\epsilon} \text{ with } \boldsymbol{\epsilon} \sim \mathcal{N}(\mathbf{0}, \mathbf{I}) \tag{2.4}$$

   where $[\boldsymbol{\theta}^{(r-1)\prime}\ \mathbf{s}^{(r-1)\prime}]^\prime$ is the previously accepted draw of $[\boldsymbol{\theta}^\prime\ \mathbf{s}^\prime]^\prime$ and c is an scale constant selected to achieve a acceptance ratio of 25 percent.

3. Set $[\boldsymbol{\theta}^{(r)\prime}\ \mathbf{s}^{(r)\prime}]^\prime = [\boldsymbol{\theta}^{*\prime}\ \mathbf{s}^{*\prime}]^\prime$ with probability 'α' or $[\boldsymbol{\theta}^{(r)\prime}\ \mathbf{s}^{(r)\prime}]^\prime = [\boldsymbol{\theta}^{(r-1)\prime}\ \mathbf{s}^{(r-1)\prime}]^\prime$ with probability '$1 - \alpha$'. The MH likelihood, α, is computed according to

$$\alpha = \min\left\{1, \frac{p(\mathbf{s}^*, \boldsymbol{\theta}^* | \mathbf{y})}{p(\mathbf{s}^{(r-1)}, \boldsymbol{\theta}^{(r-1)} | \mathbf{y})}\right\}. \tag{2.5}$$

4. If $r \leq B$ repeat steps 2 and 3 otherwise continue to the next step.

5. With $[\boldsymbol{\theta}^{(r)\prime}\ \mathbf{s}^{(r)\prime}]^\prime$ compute all of the required moment transformations. For instance, $IRF^{(r)}$, $\boldsymbol{\alpha}^{(r)}$, etc.

6. If $r < B + R$ repeat (2-5), otherwise, integrate $\left\{\boldsymbol{\theta}^{(r)},\ \mathbf{s}^{(r)},\ IRF^{(r)}, \boldsymbol{\alpha}^{(r)},\ \ldots\right\}_{r=B+1}^{B+R}$ via Monte Carlo.

[5] In Lenza and Primiceri (2022), $p(\mathbf{s})$ is formulated using a Pareto distribution consistent with extreme values.

3 An application

To evaluate the performance of the variation to the Kalman Filter recursion proposed in Section 2, a model based on HLW2020 is introduced. It should be noted that, although under specific calibration, the subsequent model simplifies to the exact model used in HLW2020, it does not guarantee that their results can be replicated. This discrepancy arises because HLW2020 implements a sequential multi-step approach in the estimation process, whereas this paper conducts the estimation jointly. Another aspect to consider when discerning the differences is that HLW2020 employs a frequentist approach for model estimation, while this paper adopts a Bayesian approach.

Another important consideration is that the primary objective of this estimation is to assess the performance of the proposed algorithm, rather than to construct a rigorous estimate of the relevant non-observables in the model. Given that the model employed is a straightforward extension of the canonical New Keynesian model, as seen in the works of Woodford (1999), Galí (2015) and Walsh (2017), it would be unrealistic to assert that these estimates can be regarded as rigorous estimations for the US, CA, and the EA. Consequently, the emphasis is placed on the quality of the estimation and the necessary adjustments during the filtering process.

3.1 A local-level model based on HLW2020

The initial step in describing the model corresponds to the characterization of GDP. It is assumed that GDP, denoted as y^{obs}, can be decomposed in a non-inflationary trend, $\bar{y}$, and an output-gap, $\hat{y}$. This assumption is incorporated into the measurable equation 3.1, where a measurement error, ϵ^y, is included.[6]

$$y_t^{obs} = \bar{y}_t + \hat{y}_t + \epsilon_t^y. \tag{3.1}$$

The non-inflationary trend of GDP evolves according to the Clark model, i.e., it is an $I(2)$ process where the drift, $\bar{g}$, is a random walk itself as display in equations 3.2 and 3.3. This drift can also be understood a the long-run growth rate of GDP, as a result it is also a determinant of the neutral interest rate as it will be assumed in equation 3.12.

$$\bar{y}_t = \bar{y}_{t-1} + \bar{g}_{t-1} + \varepsilon_t^{\bar{y}} \text{ with } \varepsilon_t^{\bar{y}} \overset{iid}{\sim} \mathcal{N}(0, \kappa_{\bar{y},t}^2 q_{\bar{y}}^2) \text{ and} \tag{3.2}$$

$$\bar{g}_t = \bar{g}_{t-1} + \varepsilon_t^{\bar{g}} \text{ with } \varepsilon_t^{i} \overset{iid}{\sim} \mathcal{N}(0, q_{\bar{g}}^2). \tag{3.3}$$

It should be noted that the state shock, $\varepsilon_t^{\bar{y}}$, is presumed to be influenced by the sudden surge in volatility stemming from the pandemic. The increment in volatility is regulated by $\kappa_{\bar{y},t}$, which is designed to exhibit the behavior described in 2.2. To facilitate the estimation process and to avoid the piled-up problem, it is assumed that $q_{\bar{y}} = \frac{\lambda_{\bar{y}}}{100} q_{\hat{y}}$ and $\kappa_{\bar{y},t} = 1 + 100\frac{\tilde{\kappa}_{\bar{y},t}}{q_{\bar{y}}}$, where $\lambda_{\bar{y}}$ and $\tilde{\kappa}_{\bar{y},t}$ are the actual parameters to be estimated.[7]

As shown in Equation 3.4, the output gap, $\hat{y}$, is driven by a clear New Keynesian rationale. It is determined by an 'expectations component', $a_y\left(a_{y1}\hat{y}_{t-1} + a_{y2}\hat{y}_{t-2}\right) + (1-a_y)\mathrm{E}_t\hat{y}_{t+1}$, and by 'financial conditions', $(1-a_{\psi 1})\psi_t + a_{\psi 1}(1-a_{\psi 2})\psi_{t-1} + a_{\psi 1}a_{\psi 2}\psi_{t-2}$. Similar to the state shock for trend GDP, the output gap shock, $\varepsilon_t^{\hat{y}}$, also exhibits a nonlinear behavior in which the variance is modulated by $\kappa_{\hat{y},t}$, which evolves according to 2.2.

$$\begin{aligned}\hat{y}_t =& a_{ye}\left[a_y\left(a_{y1}\hat{y}_{t-1} + a_{y2}\hat{y}_{t-2}\right) + (1-a_y)\mathrm{E}_t\hat{y}_{t+1}\right] \ \ldots \\ & - a_\psi\left[(1-a_{\psi 1})\psi_t + a_{\psi 1}(1-a_{\psi 2})\psi_{t-1} + a_{\psi 1}a_{\psi 2}\psi_{t-2}\right] + \varepsilon_t^{y} \text{ with } \varepsilon_t^{\hat{y}} \overset{iid}{\sim} \mathcal{N}(0, \kappa_{\hat{y},t}^2 q_{\hat{y}}^2),\end{aligned} \tag{3.4}$$

[6] The standard error of all measurement errors is calibrated to be 10 percent of the standard deviation of their corresponding measurement variable (or its growth rate, in the case of non-stationarity).

[7] All priors are displayed in tables 2, 3 and 4. In the particular case of the $\kappa_{j,t}$ coefficients, all of those are formulated with a diffuse prior (especifically: $\Gamma^{-1}(10;10)$).

where $a_{y1} = 2\omega_1 \cos\left[\frac{\pi}{20} + \omega_2\left(\frac{\pi}{3} - \frac{\pi}{20}\right)\right]$, $a_{y2} = -\omega_1^2$ and $\omega_1, \omega_2, a_\psi, a_{\psi 1}, a_{\psi 2} \in [0,\ 1]$. As in the case of the output trend shock, it is assumed that $\kappa_{\hat{y},t} = 1 + \frac{\tilde{\kappa}_{\hat{y},t}}{q_{\hat{y}}}$, where $\tilde{\kappa}_{\hat{y},t}$ represents the actual parameter to be estimated.

Within the 'financial conditions' expression in equation 3.4, ψ represents the deviations of the ex-ante real interest rate from is neutral counterpart, $\bar{r}$. As shown in equation 3.5, the ex-ante real interest rate is calculated as the difference between the nominal interest rate, i_t, and inflation expectations, $\mathrm{E}_t\pi_{t+1}$.

$$\psi_t = i_t - \mathrm{E}_t\pi_{t+1} - \bar{r}_t \tag{3.5}$$

The behavior of the inflation rate is based upon the structure of a Phillips curve with price indexation within a New Keynesian model. Given that the length of the sample used may align with changes in inflation intercepts over time, the observed inflation, π^{obs}, is modeled using the subsequent measurement equation:

$$\pi_t^{obs} = \bar{\pi}_t + \hat{\pi}_t + \epsilon_t^{\pi}, \tag{3.6}$$

where $\bar{\pi}$, $\hat{\pi}$, and ϵ^{π} represent the time-varying inflation intercept, the cyclical inflation rate and the measurement error, respectively. The inflation intercept evolves according to a random walk as shown in 3.7,

$$\bar{\pi}_t = \bar{\pi}_{t-1} + \varepsilon_t^{\bar{\pi}} \text{ with } \varepsilon_t^i \overset{iid}{\sim} \mathcal{N}(0, q_{\bar{\pi}}^2), \tag{3.7}$$

where $q_{\bar{\pi}} = \frac{\lambda_{\bar{\pi}}}{25} q_{\hat{\pi}}$ where $\lambda_{\bar{\pi}}$ will be estimated.

The cyclical component of inflation is assumed to follow a similar structure as a Phillip curve with indexation as displayed in equation 3.8. The 'expectation component' of this equation is represented by $b_{\pi 0} b_\pi \hat{\pi}_{t-1} + (1 - b_\pi)\mathrm{E}_t\hat{\Pi}_{t+4}$ while the demand component is set by $(1 - b_{y1})\hat{y}_t + b_{y1}(1 - b_{y2})\hat{y}_{t-1} + b_{y1}b_{y2}\hat{y}_{t-2}$,

$$\begin{aligned} \hat{\pi}_t =& b_{\pi 0} b_\pi \hat{\pi}_{t-1} + (1 - b_\pi)\mathrm{E}_t\hat{\Pi}_{t+4} \ ... \\ &+ b_y\left[(1 - b_{y1})\hat{y}_t + b_{y1}(1 - b_{y2})\hat{y}_{t-1} + b_{y1}b_{y2}\hat{y}_{t-2}\right] + \varepsilon_t^{\hat{\pi}} \text{ with } \varepsilon_t^{\hat{\pi}} \overset{iid}{\sim} \mathcal{N}(0, q_{\hat{\pi}}^2), \end{aligned} \tag{3.8}$$

where $b_{\pi 0}, b_\pi, b_y, b_{y1}, b_{y2} \in [0, 1]$. The term Π denotes the year-on-year inflation rate, while $\hat{\Pi}$ represent its deviation from the corresponding intercept. These terms are displayed in the following equation:

$$\Pi_t = \frac{\pi_t + \pi_{t-1} + \pi_{t-2} + \pi_{t-3}}{4} \text{ and } \hat{\Pi}_t = \frac{\hat{\pi}_t + \hat{\pi}_{t-1} + \hat{\pi}_{t-2} + \hat{\pi}_{t-3}}{4}. \tag{3.9}$$

With regard to the interest rate, HLW2020 formulates the state space representation in such a way that the model remains agnostic about the determinants of the interest rate. In the model introduced here, the interest rate is assumed to adhere to a behavior derived from a flexible Taylor rule. The measurement equation for the interest rate is as follows:

$$i_t^{obs} = i_t + \epsilon_t^i. \tag{3.10}$$

The Taylor rule is then given by 3.11. This equation incorporates the standard New Keynesian components: expected inflation deviations, $\mathrm{E}_t\hat{\Pi}_{t+4}$, and excess demand, $f_{y1}\hat{y}_{t-1} + (1 - f_{y1})\hat{y}_t$.

$$\begin{aligned} i_t =& \rho_i i_{t-1} + (1 - \rho_i)\left[(\bar{r}_t + \bar{\pi}_t) + (1 + f_\pi)\mathrm{E}_t\hat{\Pi}_{t+4} + f_y(f_{y1}\hat{y}_{t-1} + (1 - f_{y1})\hat{y}_t)\right] + \varepsilon_t^i \\ &\text{with } \varepsilon_t^i \overset{iid}{\sim} \mathcal{N}(0, q_i^2), \end{aligned} \tag{3.11}$$

where $\rho_i, b_\pi, f_\pi, b_{y1}, f_y, f_{y1} \in [0, 1]$.

As in HLW2020 and and as depicted in equation 3.12, the neutral real interest rate, $\bar{r}$, has two components. The long-run growth rate of GDP, $\bar{g}$, and a non-observable variable $\bar{z}$ which represents the systematic financial conditions within the system. The latter variable follows a random walk process as shown in 3.13,

$$\bar{r}_t = \bar{g}_t + \bar{z}_t \text{ and} \tag{3.12}$$

$$\bar{z}_t = \bar{z}_{t-1} + \varepsilon_t^{\bar{z}} \text{ with } \varepsilon_t^{\bar{z}} \overset{iid}{\sim} \mathcal{N}(0, q_{\bar{z}}^2), \tag{3.13}$$

where $q_{\bar{z}} = \frac{\lambda_{\bar{s}}}{100} \frac{q_{\tilde{y}}}{a_\psi}$ to avoid the piled-up problem.

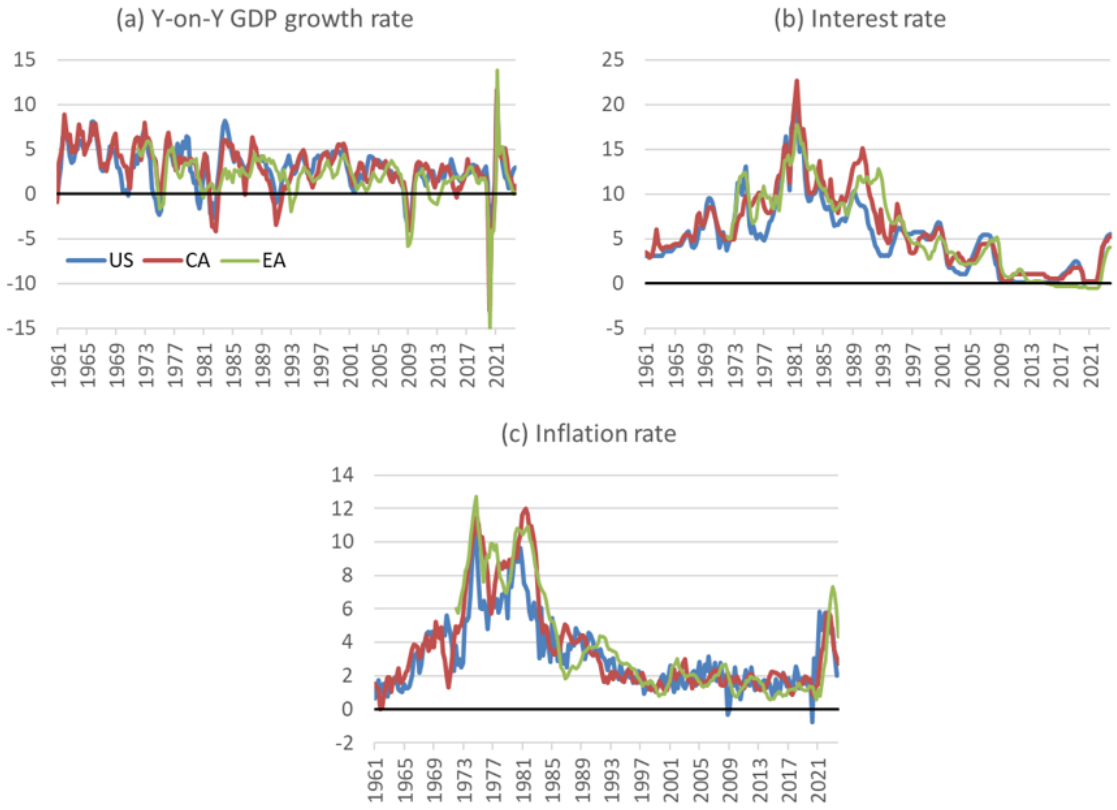

Figure 1. *Dataset from HLW2020*

The model is estimated with the dataset referenced in Holston, Laubach, and Williams (2020). This dataset comprises the logarithm of GDP (multiplied by 100), the annualized nominal short-term interest rate, and the annualized quarter-on-quarter inflation rate. Estimations for three regions are implemented: the US, CA, and the EA.[8]

All of these variables are illustrated in Figure 1. For simplicity, we display the year-on-year growth rate of GDP, even though the actual measurement variable is the logarithm of GDP. Upon a simple visual inspection, it becomes evident that the Covid-19 pandemic significantly affected the sample variability of GDP, while leaving

[8] The Federal Reserve Bank of New York regularly updates this dataset, which is accessible on their website at Measuring the Natural Rate of Interest.

the other two variables relatively unchanged.

3.2 Results

One of the concerns regarding the substantial sample variability induced by the pandemic is the potential bias it may introduce in the estimation of coefficients or in the filtering of non-observable variables. Consequently, this subsection is divided into two segments. The first pertains to the estimation of coefficients and data fit, while the second focuses on the filtering process.

3.2.1 Coefficients estimation

The estimation results are displayed in tables 2, 3 and 4 in appendix A which is also summarized in table 1. From these tables, it is evident that the estimations using the complete sample compromise the model's fit to the data, as they reduce the log data density in both the linear estimation and the estimation with the modified (corrected) algorithm. However, it is noteworthy that when the linear model is compared with the corrected model, there is, in all instances, at least a moderate improvement in the model's fit to the data.

Considering that there is no significant fluctuation in volatility within the pre-Covid-19 sample, it can serve as a benchmark for comparing the results from the estimates using the complete sample. It is noteworthy that most coefficients, especially those related to variance, undergo considerable alterations in their estimates when the complete sample is employed without any Covid-19 correction. Interestingly, when the Covid-19 correction is implemented, the deviations from the benchmark diminish, potentially indicating a reduction in bias.

Sample and algorithm		Log data density	Dev. from pre Covid-19
US	Pre Covid-19 & linear	-1283,56	
	Complete sample & linear	-1468,56	0,72
	Complete sample & corrected	-1404,54	0,62
CA	Pre Covid-19 & linear	-1404,62	
	Complete sample & linear	-1607,97	0,41
	Complete sample & corrected	-1512,27	0,10
EA	Pre Covid-19 & linear	-927,63	
	Complete sample & linear	-1223,18	0,74
	Complete sample & corrected	-1050,11	0,55

Note: The term 'Deviation from pre-Covid-19' denotes the square root of the average squared change in coefficient estimations between the model utilizing the complete sample and the model employing the pre-pandemic sample.

Table 1. *Estimation results summery*

An alternative method to evaluate the performance of the proposed approach is by examining whether the filtered shocks are effectively isolated from the Covid-19 effects. In figures 9, 10 and 11 in appendix A the left panels ((a) and (c)) display the magnitude of the Covid-19 correction to the shock (blue lines), while the right panels ((b) and (d)) show the shocks with Covid-19 effects removed. Notably, the suggested recursion successfully eliminates the pandemic effects from the filtered shocks.

Finally, the shocks designed to absorve the Covid-19 effects, $\varepsilon^{\hat{y}}$ and $\varepsilon^{\bar{y}}$, can be written as

$$\varepsilon_t^{\hat{y}} = q_{\hat{y}}\left(\mu_t^{\hat{y}} + \frac{\kappa_{\hat{y},t}}{q_{\hat{y}}}\mu_t^{\hat{y}}\right) \text{ and } \varepsilon_t^{\bar{y}} = q_{\bar{y}}\left(\mu_t^{\bar{y}} + 100\frac{\kappa_{\bar{y},t}}{q_{\bar{y}}}\mu_t^{\bar{y}}\right) \text{ with } q_{\bar{y}} = \frac{\lambda_{\bar{y}}}{100}q_{\hat{y}}, \tag{3.14}$$

where the terms $\frac{\kappa_{\hat{y},t}}{q_{\hat{y}}}\mu_t^{\hat{y}}$ and $100\frac{\kappa_{\bar{y},t}}{q_{\bar{y}}}\mu_t^{\bar{y}}$ correspond to the Covid-19 adjustments to the output gap and trend shocks, respectively. Based on the recursion described in section 2, the econometric relevance of these shocks can be evaluated for each quarter. Figure 2 presents the estimated adjustments to these shocks for each quarter, along with their credible intervals. From this figure, it can be observed that most corrections are significant from the first quarter of 2020 (20q1) to its third quarter (20q3), while none are significant in the fourth quarter (20q4). Given the lack of significant corrections at the end of 2020, no adjustments are introduced for subsequent periods.

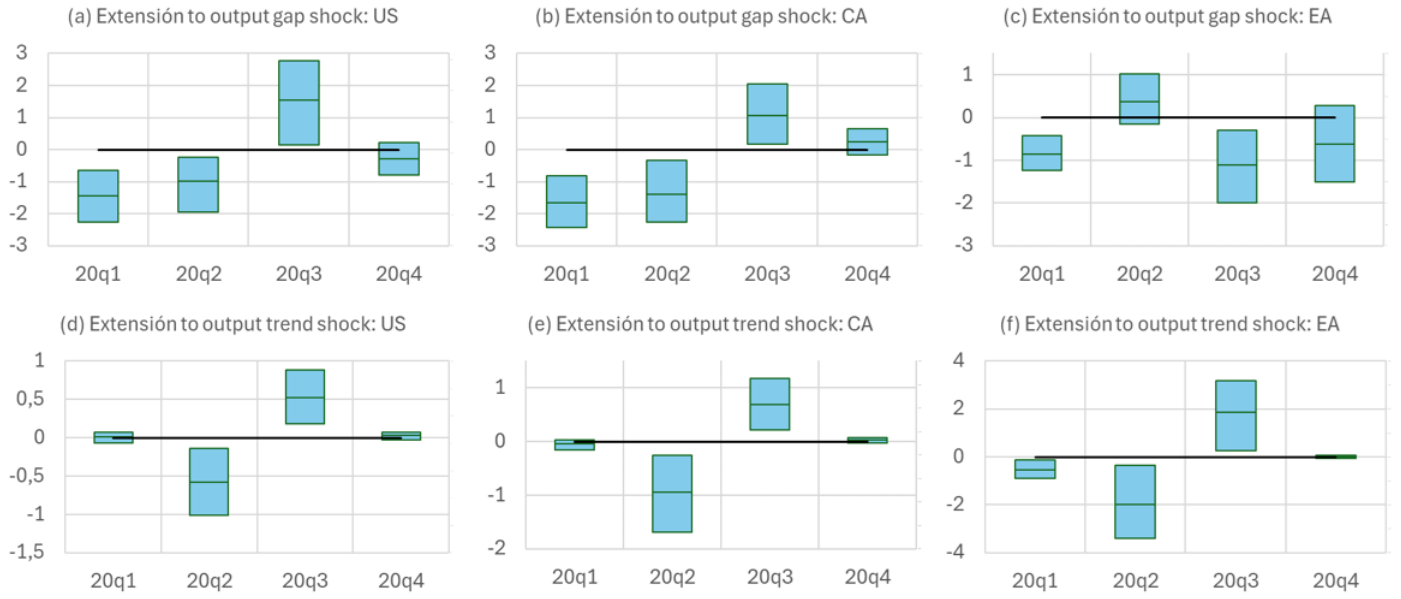

Figure 2. *Shocks' Correction for the Covid-19 event*

3.2.2 Estimation of non-observable variables

The estimation of non-observable variables for the entire sample is presented in figures 6, 7 and 8 in appendix A for the US, CA and EA, respectively. This section specifically focuses on the filtering around the year 2020. Consequently, figures 3, 4 and 5 displays the estimations of the relevant non-observable variables for the US, CA and EA, respectively. In all of these charts, the following estimations are presented: the linear estimation using the pre-Covid-19 sample (represented by green lines), the linear estimation using the complete sample (represented by blue lines), and the variance-corrected estimation using the complete sample (represented by red lines).

The first notable observation is that the absence of COVID-19 correction appears to underestimate the uncertainty during and after the pandemic. This is evident in the significantly larger amplitude of the red line bands compared to the alternative linear estimation. This pattern is consistent across all countries and variables. For the output gap and trend inflation—variables adjusted in the model's design—the pre-pandemic filter (green lines) is closer to the corrected filter (red lines).

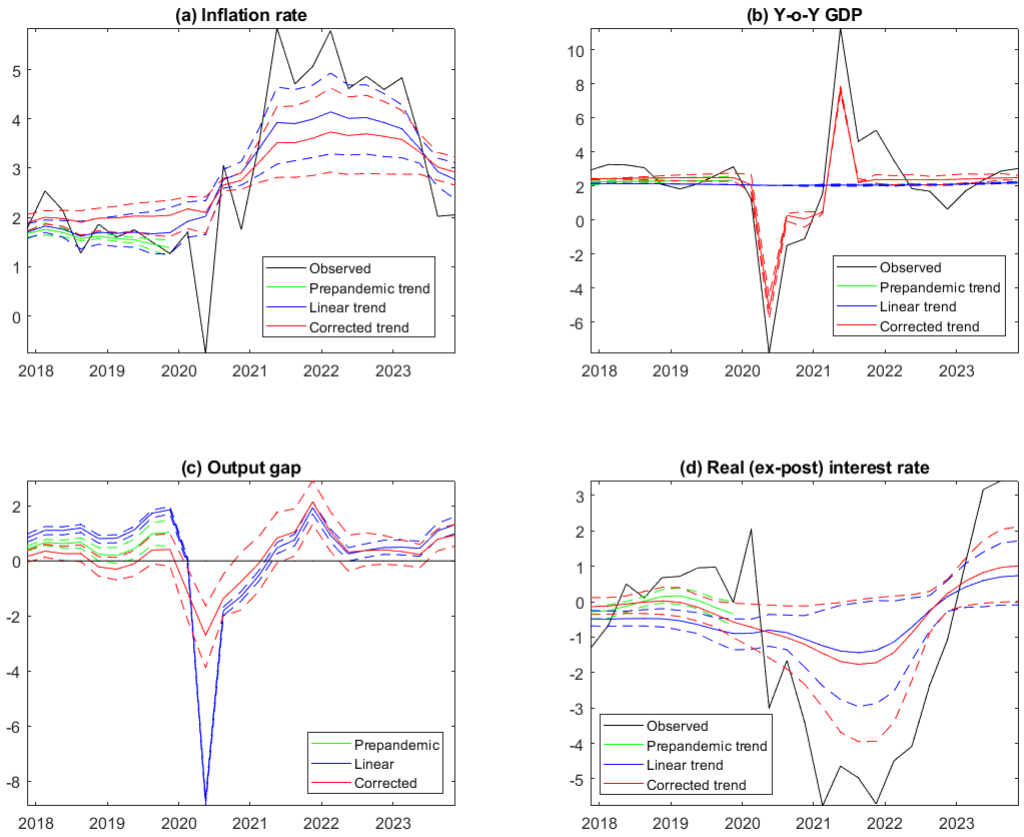

Figure 3. *US: Non-observable variables around year 2020*

Regarding the output gap, it is evident that the linear filter significantly overestimates the effects of the pandemic, which is counterbalanced by a substantial positive output gap prior to it (blue lines). When the COVID-19 correction is applied, the contraction in 2020 is moderated, albeit with an increase in uncertainty. This trend aligns with the price evolution during that period, which does not exhibit abnormal variation. Additionally, it is noteworthy that, in all scenarios, output gap from 2022 onwards show signs of convergence among alternative estimations.

One of the key differences between the linear and COVID-19 corrected estimations lies in the assessment of output trends. Three common observations emerge across estimations for all countries:

- Most of the impact of the pandemic is absorbed by the level of trending output, $\bar{y}$, rather than its long-run growth rate, $\bar{g}$. The latter eventually decreases but in a more gradual manner.
- Uncertainty increases considerably following the pandemic.
- The linear estimation entirely isolates the trend from the effects of the pandemic.

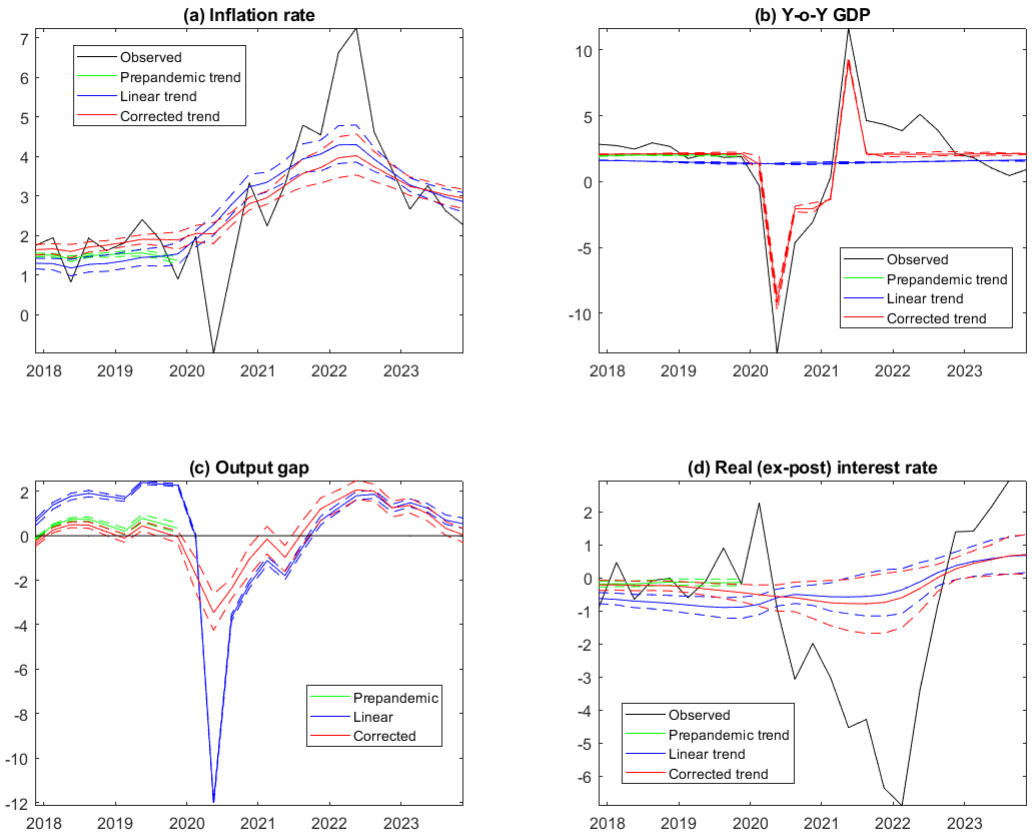

Figure 4. *CA: Non-observable variables around year 2020*

In the context of the neutral interest rate, the Covid-19 adjusted model exhibits behavior comparable to the linear estimation within the pre-pandemic sample. Post-2020, a prolonged contraction is observed for this non-observable variable. Although the linear filter applied to the complete sample yields similar neutral rates on average following the pandemic, the uncertainty associated with the corrected model is significantly greater.

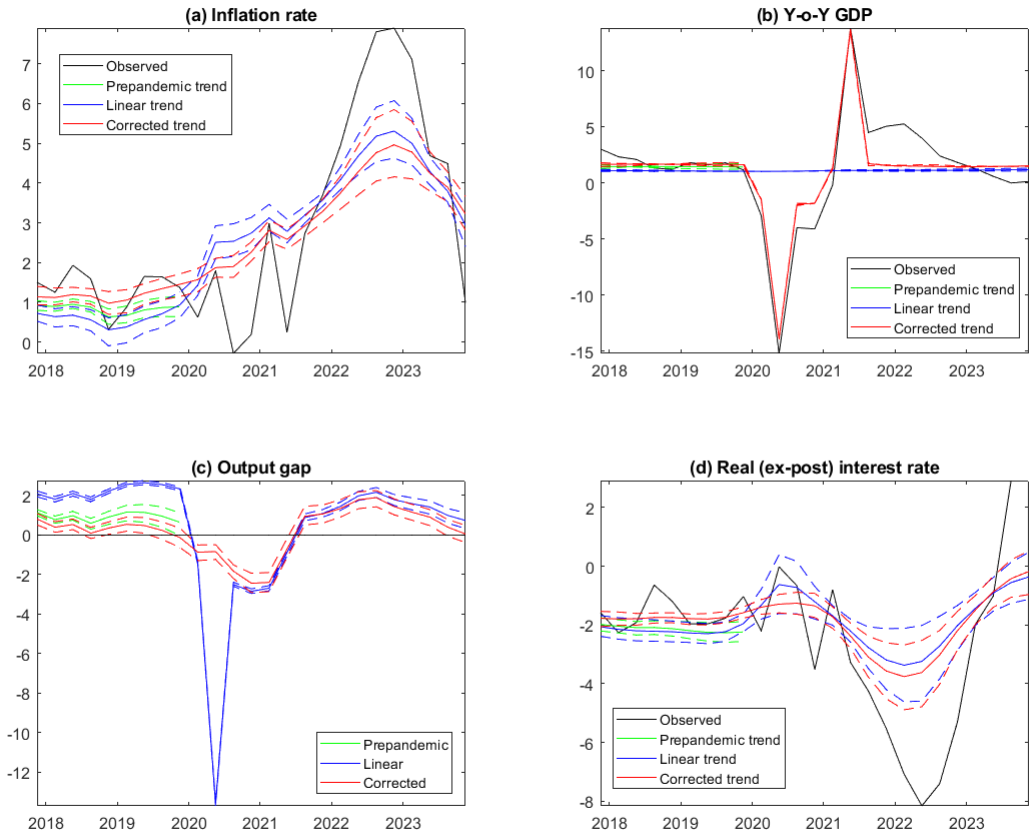

Figure 5. *EA: Non-observable variables around year 2020*

4 Conclusions

In this paper, we develop an algorithm for structural estimation within a state-space model framework that is robust to persistent tail events, such as the Covid-19 pandemic. The fundamental concept is taken from LP2022 which posits the significant sample variation observed in 2020 should be matched with a volatility surge of some state shocks. Given that a structural model may be populated by many diferent shocks, a preliminary step involves the careful selection of specific shocks to be affected by this volatility surge.

To validate the algorithm, we construct and estimate a semi-structural model of a closed economy based on HLW2020, using the same data from the US, CA, and EA. Unlike HLW2022, our algorithm does not require additional information sources to signal the pandemic. In HLW2022 the aditional variables used is the Oxford COVID-19 government stringency index.

In the simple application implemented, we found that the proposed Covid-19 treatment enhances model fit and stabilizes coefficients. Most significant shock adjustments occurred from 2020Q1 to 2020Q3, but not in 2020Q4. Hence, the Covid-19 correction is limited to these quarters. Omitting the Covid-19 correction results in underestimated uncertainty, excessive output gap responses, inadequate output trend responses, and biased estimates of unobservable variables.

Although the application focuses on the Covid-19 pandemic, the described algorithm is useful for addressing

any event characterized by extreme variability. This proves advantageous in a changing environment marked by notable uncertainty. Considering that various events, such as major crises or climate change, could trigger significant macroeconomic fluctuations, the algorithm's generality allows its application to any structural model that can be represented within a state-space framework. Consequently, this work is important for continuing to use models designed to understand the economics surrounding us, even in the face of extreme events.

Bibliography

Beveridge, S., and C. R. Nelson (1981): "A new approach to decomposition of economic time series into permanent and transitory components with particular attention to measurement of the 'business cycle'," *Journal of Monetary economics*, 7(2), 151–174.

Carriero, A., T. E. Clark, M. Marcellino, and E. Mertens (2022): "Addressing COVID-19 outliers in BVARs with stochastic volatility," *Review of Economics and Statistics*, pp. 1–38.

Galí, J. (2015): *Monetary policy, inflation, and the business cycle: an introduction to the new Keynesian framework and its applications*. Princeton University Press.

Hale, T., S. Webster, A. Petherick, T. Phillips, and B. Kira (2020): "Oxford COVID-19 government response tracker (OxCGRT)," *Last updated*, 8, 30.

Holston, K., T. Laubach, and J. C. Williams (2017): "Measuring the natural rate of interest: International trends and determinants," *Journal of International Economics*, 108, S59–S75.

——— (2020): "Adapting the Laubach and Williams and Holston, Laubach, and Williams models to the COVID-19 pandemic," *Federal Reserve Bank of New York Note*.

Kamber, G., J. Morley, and B. Wong (2018): "Intuitive and reliable estimates of the output gap from a Beveridge-Nelson filter," *Review of Economics and Statistics*, 100(3), 550–566.

Laubach, T., and J. C. Williams (2003): "Measuring the natural rate of interest," *Review of Economics and Statistics*, 85(4), 1063–1070.

Lenza, M., and G. E. Primiceri (2022): "How to estimate a vector autoregression after March 2020," *Journal of Applied Econometrics*, 37(4), 688–699.

Morley, J., D. Rodríguez-Palenzuela, Y. Sun, and B. Wong (2023): "Estimating the euro area output gap using multivariate information and addressing the COVID-19 pandemic," *European Economic Review*, 153, 104385.

Walsh, C. E. (2017): *Monetary theory and policy*. MIT press.

Woodford, M. (1999): "Interest and prices," *manuscript, Princeton University, April*, 30(4).

A Complementary figures and tables

A.1 Coefficients estimates

Coef.	Prior			Pre Covid-19			No corrected			Corrected		
	Shape	Mean	Desv.	Mean	HPD 5%	HPD 95%	Mean	HPD 5%	HPD 95%	Mean	HPD 5%	HPD 95%
$\lambda_{\bar{\pi}}$	Γ^{-1}	5,0	1,5	13,310	6,582	20,764	16,067	6,589	24,562	12,302	6,045	19,138
$\lambda_{\bar{y}}$	Γ^{-1}	2,0	4,0	1,730	0,543	3,248	1,723	0,510	2,849	1,638	0,512	2,871
$q_{\bar{y}}$	Γ^{-1}	5,0	1,0	11,911	6,151	17,440	13,636	7,458	19,899	14,706	7,445	21,807
$\lambda_{\bar{z}}$	Γ^{-1}	2,0	4,0	2,120	0,600	3,697	1,865	0,681	3,151	2,287	0,677	4,006
a_{ye}	$\mathcal{B}$	0,5	0,2	0,971	0,947	0,996	0,950	0,910	0,993	0,968	0,943	0,996
a_y	$\mathcal{B}$	0,5	0,2	0,945	0,900	0,989	0,936	0,886	0,989	0,948	0,907	0,994
ω_1	$\mathcal{B}$	0,5	0,2	0,713	0,662	0,763	0,596	0,534	0,659	0,689	0,634	0,749
ω_2	$\mathcal{B}$	0,5	0,2	0,074	0,012	0,132	0,099	0,016	0,177	0,071	0,012	0,126
a_ψ	$\mathcal{B}$	0,5	0,2	0,085	0,023	0,150	0,162	0,041	0,295	0,132	0,026	0,225
$a_{\psi 1}$	$\mathcal{B}$	0,5	0,2	0,515	0,199	0,850	0,544	0,218	0,872	0,580	0,267	0,901
$a_{\psi 2}$	$\mathcal{B}$	0,5	0,2	0,510	0,188	0,841	0,549	0,224	0,872	0,549	0,234	0,872
$q_{\hat{y}}$	Γ^{-1}	2,0	4,0	2,810	2,514	3,108	3,960	3,559	4,344	2,718	2,432	2,989
$b_{\pi 0}$	$\mathcal{B}$	0,5	0,2	0,626	0,395	0,832	0,569	0,311	0,831	0,641	0,420	0,843
b_π	$\mathcal{B}$	0,5	0,2	0,766	0,596	0,942	0,657	0,382	0,900	0,774	0,619	0,928
b_y	$\mathcal{B}$	0,5	0,2	0,023	0,012	0,034	0,030	0,017	0,043	0,026	0,014	0,038
b_{y1}	$\mathcal{B}$	0,5	0,2	0,532	0,305	0,764	0,453	0,228	0,677	0,518	0,285	0,758
b_{y2}	$\mathcal{B}$	0,5	0,2	0,516	0,272	0,755	0,548	0,302	0,785	0,521	0,268	0,768
$q_{\bar{\pi}}$	Γ^{-1}	2,0	4,0	0,614	0,524	0,710	0,622	0,494	0,737	0,668	0,574	0,762
ρ_i	$\mathcal{B}$	0,5	0,2	0,616	0,467	0,764	0,767	0,651	0,878	0,747	0,591	0,882
f_π	Γ^{-1}	1,0	2,0	0,810	0,246	1,445	0,950	0,280	1,728	0,804	0,282	1,340
f_y	Γ^{-1}	0,5	2,0	0,175	0,124	0,228	0,235	0,130	0,347	0,217	0,128	0,313
f_{y1}	$\mathcal{B}$	0,5	0,2	0,437	0,203	0,647	0,372	0,165	0,575	0,403	0,173	0,643
q_i	Γ^{-1}	2,0	4,0	0,698	0,576	0,815	0,792	0,681	0,905	0,774	0,633	0,899
$\kappa_{\hat{y},20q1}$	Γ^{-1}	10,0	10,0							6,993	3,438	10,647
$\kappa_{\hat{y},20q2}$	Γ^{-1}	10,0	10,0							6,979	3,221	11,205
$\kappa_{\hat{y},20q3}$	Γ^{-1}	10,0	10,0							7,349	3,359	11,457
$\kappa_{\hat{y},20q4}$	Γ^{-1}	10,0	10,0							6,896	3,095	10,539
$\kappa_{\bar{y},20q1}$	Γ^{-1}	10,0	10,0							7,395	2,970	12,645
$\kappa_{\bar{y},20q2}$	Γ^{-1}	10,0	10,0							7,106	2,999	12,335
$\kappa_{\bar{y},20q3}$	Γ^{-1}	10,0	10,0							7,042	3,024	11,079
$\kappa_{\bar{y},20q4}$	Γ^{-1}	10,0	10,0							6,903	2,963	10,935
Dev. from pre Covid-19 estimates								0,72			0,62	
Log data density					-1283,56			-1468,56			-1404,54	

Table 2. *Estimates with US data in different samples*

Coef.	Prior			Pre Covid-19			No corrected			Corrected		
	Shape	Mean	Desv.	Mean	HPD 5%	HPD 95%	Mean	HPD 5%	HPD 95%	Mean	HPD 5%	HPD 95%
$\lambda_{\bar{\pi}}$	Γ^{-1}	5,0	1,5	10,918	7,553	14,384	11,704	8,151	15,235	10,854	7,657	14,336
$\lambda_{\bar{y}}$	Γ^{-1}	2,0	4,0	1,828	0,522	3,306	1,741	0,513	3,448	1,807	0,503	3,315
$q_{\bar{g}}$	Γ^{-1}	5,0	1,0	14,822	8,639	21,038	15,004	8,746	21,436	15,047	9,291	20,559
$\lambda_{\bar{z}}$	Γ^{-1}	2,0	4,0	2,727	0,710	4,881	2,113	0,689	3,754	3,141	0,587	5,915
a_{ye}	$\mathcal{B}$	0,5	0,2	0,961	0,930	0,995	0,937	0,885	0,993	0,965	0,933	0,996
a_y	$\mathcal{B}$	0,5	0,2	0,940	0,893	0,991	0,919	0,857	0,986	0,943	0,898	0,990
ω_1	$\mathcal{B}$	0,5	0,2	0,684	0,631	0,741	0,551	0,488	0,617	0,667	0,608	0,719
ω_2	$\mathcal{B}$	0,5	0,2	0,081	0,015	0,143	0,125	0,024	0,219	0,089	0,013	0,159
a_ψ	$\mathcal{B}$	0,5	0,2	0,150	0,037	0,279	0,187	0,056	0,313	0,157	0,035	0,275
$a_{\psi 1}$	$\mathcal{B}$	0,5	0,2	0,550	0,240	0,894	0,572	0,258	0,904	0,573	0,231	0,877
$a_{\psi 2}$	$\mathcal{B}$	0,5	0,2	0,530	0,182	0,840	0,553	0,233	0,866	0,539	0,226	0,875
$q_{\hat{y}}$	Γ^{-1}	2,0	4,0	2,875	2,559	3,204	4,526	4,064	4,971	2,759	2,499	3,038
$b_{\pi 0}$	$\mathcal{B}$	0,5	0,2	0,379	0,184	0,581	0,431	0,213	0,642	0,407	0,221	0,606
b_π	$\mathcal{B}$	0,5	0,2	0,606	0,387	0,852	0,509	0,272	0,745	0,595	0,376	0,834
b_y	$\mathcal{B}$	0,5	0,2	0,051	0,027	0,072	0,052	0,032	0,072	0,052	0,030	0,074
b_{y1}	$\mathcal{B}$	0,5	0,2	0,556	0,320	0,793	0,483	0,253	0,712	0,537	0,310	0,778
b_{y2}	$\mathcal{B}$	0,5	0,2	0,489	0,253	0,745	0,470	0,237	0,711	0,478	0,235	0,736
$q_{\bar{\pi}}$	Γ^{-1}	2,0	4,0	1,092	0,978	1,210	1,072	0,957	1,185	1,102	0,986	1,220
ρ_i	$\mathcal{B}$	0,5	0,2	0,762	0,666	0,876	0,809	0,732	0,885	0,803	0,726	0,884
f_π	Γ^{-1}	1,0	2,0	1,004	0,222	2,498	0,849	0,248	1,454	0,913	0,261	1,689
f_y	Γ^{-1}	0,5	2,0	0,194	0,123	0,266	0,224	0,131	0,313	0,215	0,134	0,304
f_{y1}	$\mathcal{B}$	0,5	0,2	0,473	0,239	0,720	0,428	0,204	0,636	0,455	0,208	0,688
q_i	Γ^{-1}	2,0	4,0	0,759	0,669	0,866	0,779	0,703	0,862	0,771	0,691	0,856
$\kappa_{\hat{y},20q1}$	Γ^{-1}	10,0	10,0							7,283	3,213	11,205
$\kappa_{\hat{y},20q2}$	Γ^{-1}	10,0	10,0							7,503	3,267	11,448
$\kappa_{\hat{y},20q3}$	Γ^{-1}	10,0	10,0							8,135	3,274	13,496
$\kappa_{\hat{y},20q4}$	Γ^{-1}	10,0	10,0							7,161	2,964	11,276
$\kappa_{\bar{y},20q1}$	Γ^{-1}	10,0	10,0							6,479	3,168	10,056
$\kappa_{\bar{y},20q2}$	Γ^{-1}	10,0	10,0							6,845	3,029	10,852
$\kappa_{\bar{y},20q3}$	Γ^{-1}	10,0	10,0							6,703	3,006	10,175
$\kappa_{\bar{y},20q4}$	Γ^{-1}	10,0	10,0							8,621	2,642	16,227
Dev. from pre Covid-19 estimates								0,41			0,10	
Log data density					-1404,62			-1607,97			-1512,27	

Table 3. *Estimates with CA data in different samples*

Coef.	Prior			Pre Covid-19			No corrected			Corrected		
	Shape	Mean	Desv.	Mean	HPD 5%	HPD 95%	Mean	HPD 5%	HPD 95%	Mean	HPD 5%	HPD 95%
$\lambda_{\bar{\pi}}$	Γ^{-1}	5,0	1,5	16,248	11,797	21,388	16,706	10,564	22,577	14,799	9,797	19,918
$\lambda_{\bar{y}}$	Γ^{-1}	2,0	4,0	2,042	0,487	4,439	1,726	0,507	3,235	2,008	0,478	4,341
$q_{\bar{g}}$	Γ^{-1}	5,0	1,0	9,891	4,890	15,051	8,685	5,191	12,444	12,061	5,406	18,792
$q_{\bar{z}}$	Γ^{-1}	2,0	4,0	2,690	0,710	4,993	4,168	0,739	8,383	3,171	0,663	10,852
a_{ye}	$\mathcal{B}$	0,5	0,2	0,972	0,948	0,996	0,909	0,835	0,984	0,964	0,933	0,995
a_y	$\mathcal{B}$	0,5	0,2	0,943	0,893	0,989	0,903	0,828	0,983	0,945	0,900	0,992
ω_1	$\mathcal{B}$	0,5	0,2	0,752	0,698	0,805	0,513	0,441	0,585	0,716	0,648	0,781
ω_2	$\mathcal{B}$	0,5	0,2	0,069	0,011	0,124	0,150	0,032	0,267	0,077	0,012	0,139
a_ψ	$\mathcal{B}$	0,5	0,2	0,108	0,024	0,204	0,284	0,049	0,548	0,188	0,029	0,392
$a_{\psi 1}$	$\mathcal{B}$	0,5	0,2	0,521	0,197	0,844	0,594	0,285	0,916	0,585	0,273	0,915
$a_{\psi 2}$	$\mathcal{B}$	0,5	0,2	0,521	0,214	0,858	0,537	0,212	0,873	0,553	0,239	0,895
$q_{\hat{y}}$	Γ^{-1}	2,0	4,0	1,984	1,757	2,230	4,914	4,389	5,473	1,912	1,667	2,153
$b_{\pi 0}$	$\mathcal{B}$	0,5	0,2	0,321	0,140	0,506	0,408	0,186	0,625	0,389	0,194	0,590
b_π	$\mathcal{B}$	0,5	0,2	0,643	0,445	0,842	0,620	0,385	0,841	0,663	0,489	0,858
b_y	$\mathcal{B}$	0,5	0,2	0,080	0,051	0,110	0,065	0,039	0,087	0,090	0,056	0,123
b_{y1}	$\mathcal{B}$	0,5	0,2	0,564	0,340	0,797	0,669	0,468	0,864	0,555	0,334	0,768
b_{y2}	$\mathcal{B}$	0,5	0,2	0,479	0,228	0,708	0,428	0,210	0,649	0,471	0,240	0,716
$q_{\hat{\pi}}$	Γ^{-1}	2,0	4,0	0,679	0,585	0,767	0,757	0,648	0,870	0,759	0,662	0,860
ρ_i	$\mathcal{B}$	0,5	0,2	0,676	0,605	0,756	0,765	0,689	0,840	0,758	0,695	0,828
f_π	Γ^{-1}	1,0	2,0	0,547	0,267	0,839	0,585	0,258	0,902	0,578	0,253	0,936
f_y	Γ^{-1}	0,5	2,0	0,173	0,122	0,223	0,142	0,095	0,183	0,166	0,109	0,220
f_{y1}	$\mathcal{B}$	0,5	0,2	0,527	0,299	0,780	0,532	0,322	0,745	0,507	0,253	0,747
q_i	Γ^{-1}	2,0	4,0	0,428	0,366	0,493	0,475	0,388	0,559	0,446	0,372	0,520
$\kappa_{\hat{y},20q1}$	Γ^{-1}	10,0	10,0							6,304	3,081	9,413
$\kappa_{\hat{y},20q2}$	Γ^{-1}	10,0	10,0							6,478	3,285	9,747
$\kappa_{\hat{y},20q3}$	Γ^{-1}	10,0	10,0							6,856	3,252	10,792
$\kappa_{\hat{y},20q4}$	Γ^{-1}	10,0	10,0							6,679	2,989	10,088
$\kappa_{\bar{y},20q1}$	Γ^{-1}	10,0	10,0							8,346	2,857	15,460
$\kappa_{\bar{y},20q2}$	Γ^{-1}	10,0	10,0							6,674	3,286	10,364
$\kappa_{\bar{y},20q3}$	Γ^{-1}	10,0	10,0							7,213	3,073	11,461
$\kappa_{\bar{y},20q4}$	Γ^{-1}	10,0	10,0							6,836	3,176	11,120
Dev. from pre Covid-19 estimates								0,74			0,55	
Log data density					-927,63			-1223,18			-1050,11	

Table 4. *Estimates with EA data in different samples*

A.2 Filtering

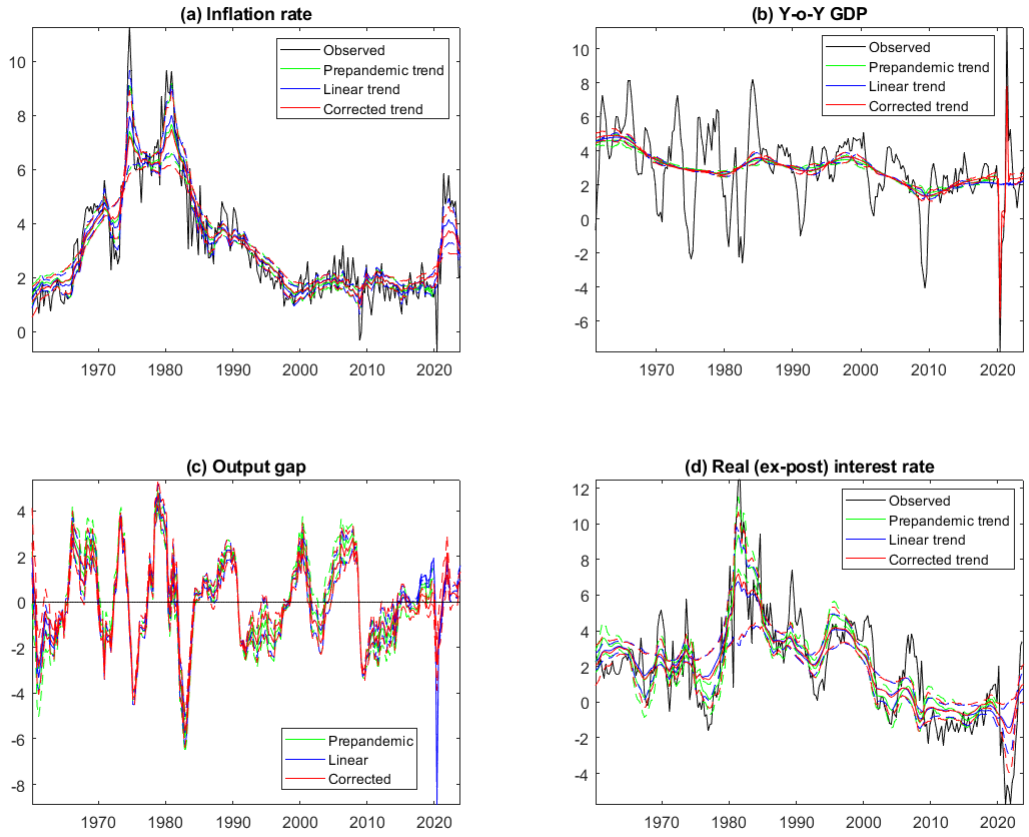

Figure 6. *US: Non-observable variables*

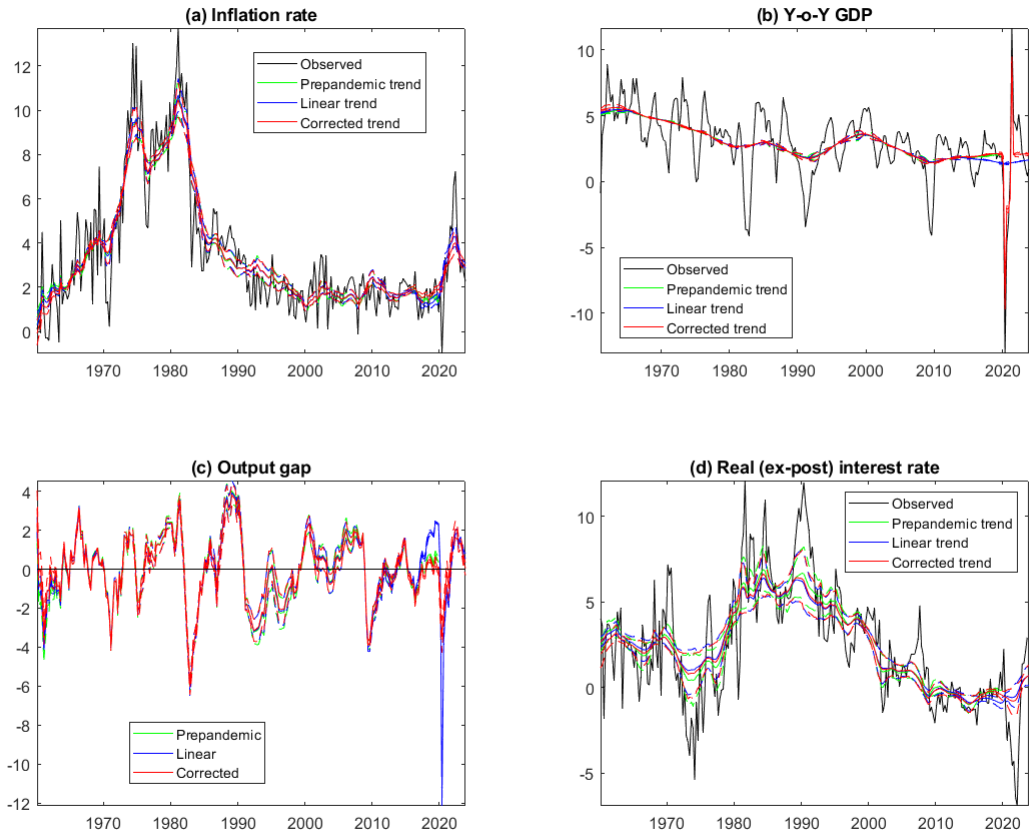

Figure 7. *CA: Non-observable variables*

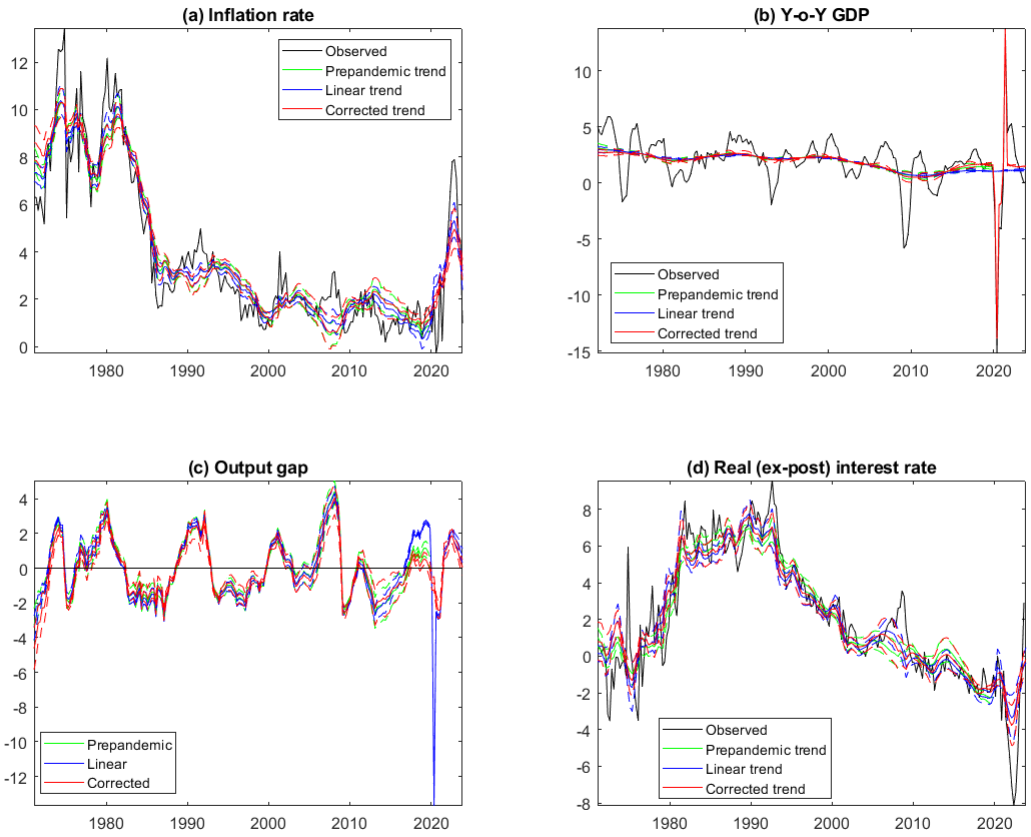

Figure 8. *EA: Non-observable variables*

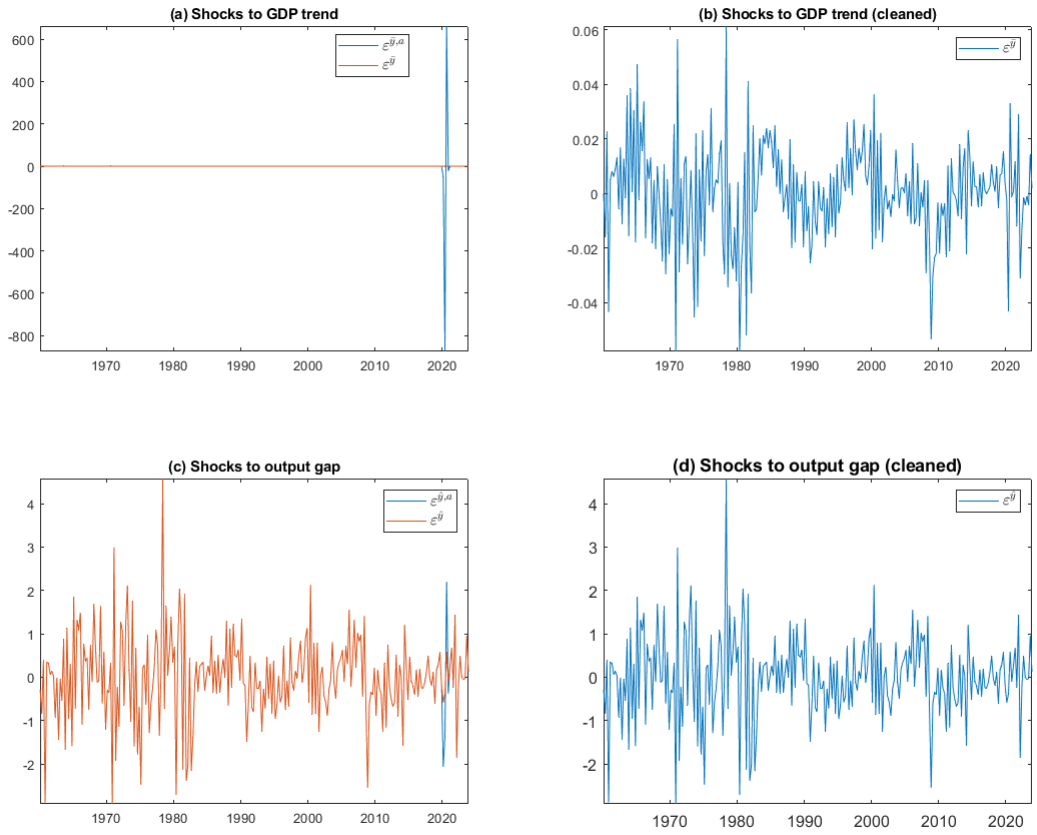

Figure 9. *US: Corrected shocks*

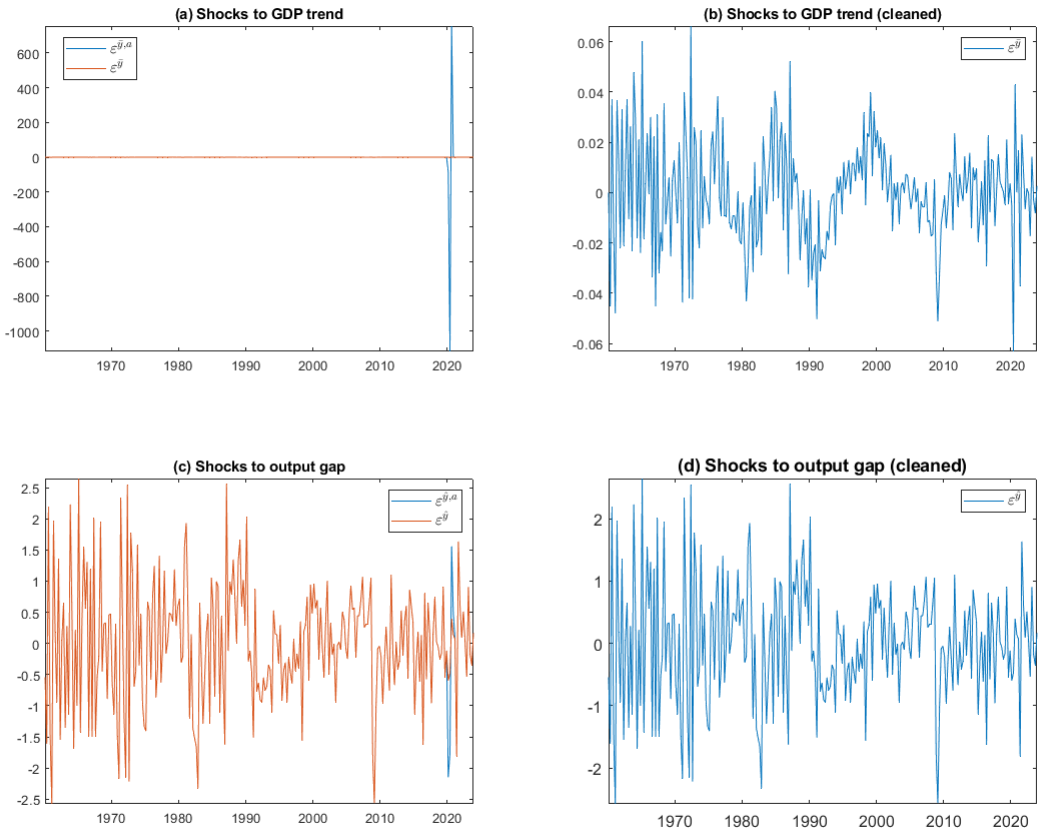

Figure 10. *CA: Corrected shocks*

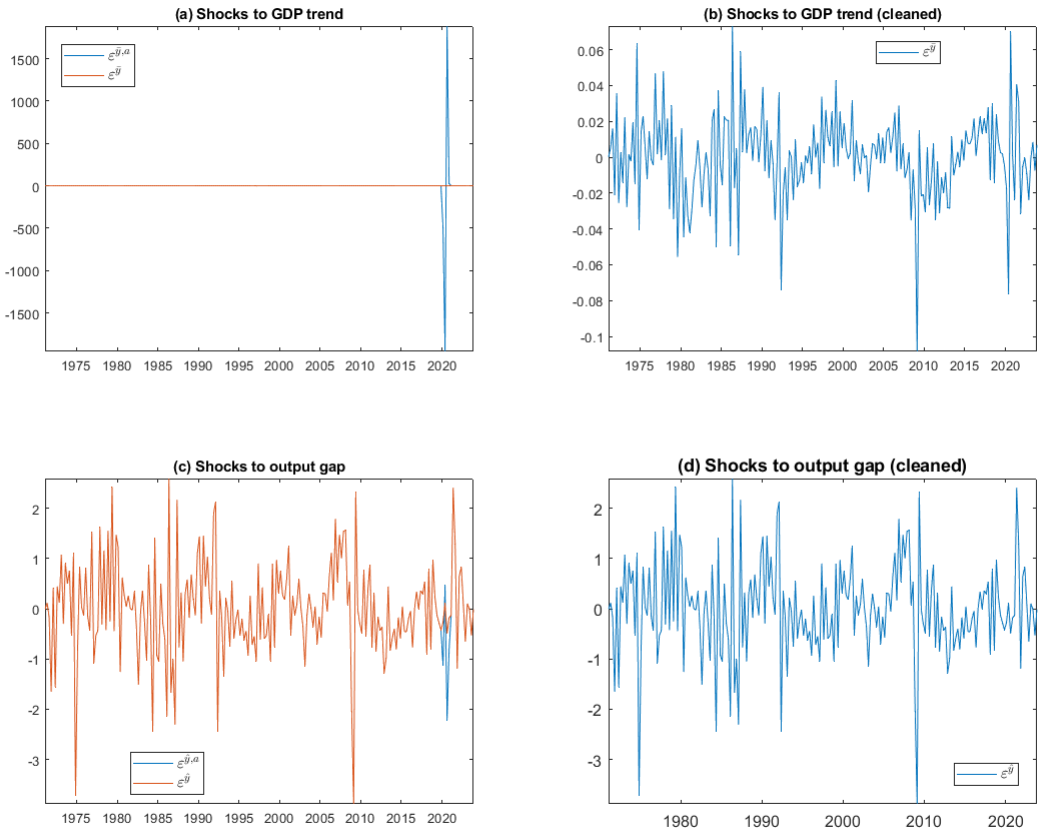

Figure 11. *EA: Corrected shocks*